A Scatterometer Geophysical Model Function for Climate-Quality Winds: QuikSCAT Ku-2011

LUCREZIA RICCIARDULLI AND FRANK J. WENTZ

Remote Sensing Systems, Santa Rosa, California

(Manuscript received 29 December 2014, in final form 5 June 2015)

ABSTRACT

Space-based observations of ocean surface winds have been available for more than 25 years. To combine the observations from multiple sensors into one record with the accuracy required for climate studies requires a consistent methodology and calibration standard for the various instruments. This study describes a new geophysical model function (GMF) specifically developed for preparing the QuikSCAT winds to serve as a backbone of an ocean vector wind climate data record. This paper describes the methodology used and presents the quality of the reprocessed winds. The new Ku-2011 model function was developed using WindSat winds as a calibration truth. An extensive validation of the Ku-2011 winds was performed that focused on 1) proving the consistency of satellite winds from different sensors at all wind speed regimes; 2) exploring and understanding possible sources of bias in the QuikSCAT retrievals; 3) validating QuikSCAT wind speeds versus in situ observations, and comparing observed wind directions versus those from numerical models; 4) comparing satellite observations of high wind speeds with measurements obtained from aircraft flying into storms; 5) analyzing case studies of satellite-based observations of winds in tropical storms; and 6) illustrating how rain impacts QuikSCAT wind speed retrievals. The results show that the reprocessed QuikSCAT data are greatly improved in both speed and direction at high winds. Finally, there is a discussion on how these QuikSCAT results fit into a long-term effort toward creating a climate data record of ocean vector winds.

1. Introduction

Satellite ocean winds are a valuable resource for weather forecasting and climate research, as winds at the ocean surface are the main drivers of atmospheric and oceanic processes that determine regional weather patterns as well as long-term climate change. To date, studies using satellite winds have brought about increased understanding in air–sea interaction, heat and energy fluxes, hurricane formation and intensity, ocean wind power potential, and impact of wind variability on the global climate and water cycle (Atlas et al. 2001; Bourassa et al. 2010; Chelton et al. 2001; Chelton and Xie 2010; Katsaros et al. 2002; Kosaka 2014; Liu 2002; Liu et al. 2008; Isaksen and Stoffelen 2000; Wentz et al. 2007; Wentz and Ricciardulli 2011; Xie 2004; Yueh et al. 2003).

Scatterometers (such as QuikSCAT) are particularly suited for climate studies, as they are inherently stable sensors in that they measure a ratio (backscattered radiation vs transmitted radiation) as compared to measuring an absolute quantity, and they are usually unaffected by satellite drifts or issues that affect the temporal stability of a time series.

The first space-based observations of ocean winds at a global scale were achieved in 1978 with the *Seasat* scatterometer and radiometer (Wentz et al. 1982). Despite the failing of the mission after only 3 months, *Seasat* provided the basis for successful continuous monitoring of ocean wind speeds from space by SSM/I radiometers (Wentz et al. 1986) starting in 1987 (Fig. 1), and wind vectors by scatterometers starting with the *ERS-1* in 1991 (Stoffelen and Anderson 1995). Satellite scatterometers determine ocean surface winds by measuring the backscatter from the ocean surface at microwave frequencies typically in the C band (~5 GHz) and Ku band (~13 GHz). New scatterometers at L band (~1 GHz) like *Aquarius* and the recently launched SMAP (Entekhabi et al. 2010; Yueh and Chaubell 2012) are a promising addition to the ocean vector wind missions. A list of past, current, and future C-, Ku-, and L-band scatterometer missions is presented in Fig. 1.

Corresponding author address: Lucrezia Ricciardulli, Remote Sensing Systems, 444 Tenth Street, Suite 200, Santa Rosa, CA 95401.
E-mail: ricciardulli@remss.com

DOI: 10.1175/JTECH-D-15-0008.1

© 2015 American Meteorological Society

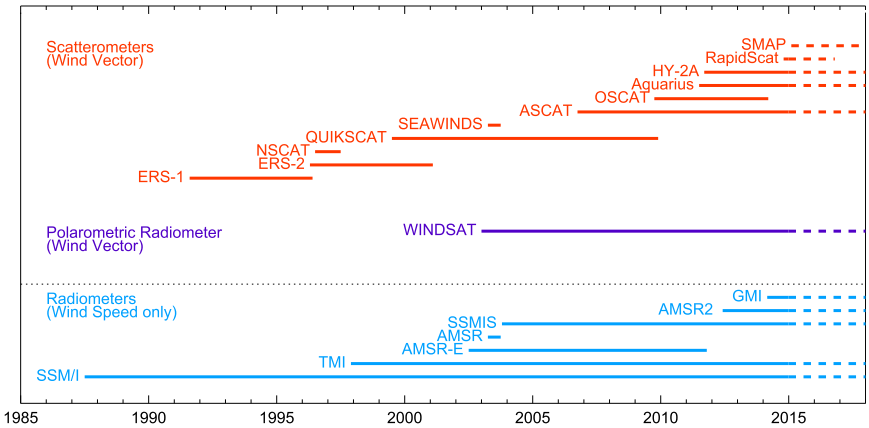

FIG. 1. Ocean surface wind satellite missions. Wind speed measurements provided by microwave radiometers (light blue) started in 1987 with the first SSM/I (*F8*). Measurements of vector winds are provided by scatterometers (red), typically at C band (ERS, ASCAT) and Ku band [NSCAT, QuikSCAT, SeaWinds, OSCAT, *Haiyang-2A* (*HY-2A*), RapidScat]. New scatterometers operate also at L band (*Aquarius*, SMAP). QuikSCAT represents the longest scatterometer mission, from 1999 to 2009. WindSat (purple) is a currently operational polarimetric radiometer that is able to measure wind direction in addition to wind speed. The dashed lines show currently operating instruments and future missions.

The longest mission so far has been the NASA Ku-band QuikSCAT (Lungu and Callahan 2006), which provided 10 continuous years (1999–2009) of ocean vector wind observations. Also in Fig. 1 are the satellite radiometer missions for wind speed.

In addition to scatterometers, a new type of radiometer, WindSat, was launched in 2003 that is capable of measuring ocean wind vectors (Gaiser et al. 2004). By using multiple polarimetric channels (10–37 GHz, plus a linearly polarized channel at 6.8 GHz), WindSat has been very successful in measuring wind direction in addition to wind speed. The scatterometers and WindSat instruments will soon provide 25 years of continuous observations that can be combined into a climate data record (CDR) of the ocean surface vector winds (OVW), if the data are consistently processed and intercalibrated.

With this goal in mind, we performed in 2011 a major reprocessing of the wind vectors from the scatterometer QuikSCAT, which we consider the backbone of the vector wind CDR. We developed a new model function for reprocessing QuikSCAT, aimed at improving the wind retrievals. Using WindSat as a calibration target, we are able to bring the scatterometer winds into alignment with radiometer wind speeds. The decade-long and still operating WindSat instrument also provides a valuable opportunity to tie together scatterometer winds from different missions [QuikSCAT, Advanced Scatterometer (ASCAT), Oceansat-2 Scatterometer (OSCAT), and the NASA scatterometer (RapidScat)]. We are also developing geophysical model functions (GMFs) for C band (ASCAT and ERS) and L band (*Aquarius* and SMAP), using calibration targets and methodologies similar to the ones described in this paper, and extending the Ku-band GMF to a wide variety of incidence angles [for NASA Scatterometer (NSCAT), OSCAT, and RapidScat]. These other GMFs will be used to reprocess 25 years of scatterometer data in a consistent way, starting with *ERS-1* in 1991.

Here we describe in detail the methodology developed for QuikSCAT processing, as it is historically the most stable and long-operating scatterometer to date. The other GMFs and the activities we perform toward development of a vector wind CDR will be the focus of future papers.

Scatterometer wind vector retrieval algorithms are based on three main components (Martin 2014): the GMF, the wind direction ambiguity removal algorithm, and the quality control. The GMF is a key component of the vector wind retrieval algorithm. It relates radar backscatter cross section σ_0 to wind speed w and the relative wind direction φ, which is defined as the wind direction minus the observing azimuth angle. The GMF is also a function of the following sensor parameters: frequency, polarization, and beam incidence angle.

The original Ku-band GMF for QuikSCAT was developed based on NSCAT data (Wentz and Smith 1999). From the NSCAT model function, two GMFs for QuikSCAT were developed independently by the NASA Jet Propulsion Laboratory (JPL) and the Remote Sensing Systems (RSS) groups. The QSCAT-1 GMF developed by Freilich and Vanhoff (1999) was

used in the operational processing of QuikSCAT wind retrievals at JPL and at NOAA, and the Ku-2001 developed by Wentz was used for processing winds at RSS. When these two GMFs were developed at the beginning of the QuikSCAT mission, there was limited data available for calibrating winds above 20 m s^{-1}. The high wind regime is where the JPL and RSS QuikSCAT datasets differed most.

Satellite retrievals of high winds are challenging for two reasons. First, validation data of winds greater than 20 m s^{-1} are scarce, or are of questionable quality. Traditionally, observed winds from buoys or winds from numerical weather prediction (NWP) models have been used as calibration ground truth in GMF development, but their accuracy for winds above 15 m s^{-1} is degraded. Some adjustments to the GMFs at high winds can be made using airborne scanning scatterometers flying in storms (Fernandez et al. 2006). Second, observations at high winds are often contaminated by the presence of rain, and it is difficult to separate the wind and rain signals in the retrievals. Rain affects the backscatter measured by the scatterometer as shown by many (Draper and Long 2004a; Hilburn et al. 2006; Stiles and Yueh 2002; Tournadre and Quilfen 2003; Weissman and Bourassa 2008). These rain effects are difficult to model and cannot be easily removed from the measurements, although there have been some efforts at extracting wind and rain simultaneously (Draper and Long 2004b).

Ultimately, the major difficulty in calibrating a GMF lies in the choice of ground truth for high winds. In the decade since the QuikSCAT original GMFs were developed, studies have shown that retrievals at high winds by the Ku-2001 GMF were too high (Renfrew et al. 2009). In the new GMF, particular attention has been devoted to improving retrievals at high wind speeds and to separating the wind signal from the rain signal. Our choice for the GMF calibration is wind retrievals from the WindSat polarometric radiometer, available since 2003. An all-weather algorithm for WindSat was developed that was capable of global wind vector retrievals even in storm conditions (Meissner and Wentz 2009). The new algorithm uses a combination of frequency channels, including a very low-frequency C-band channel. It blends a physically based rain-free algorithm for the ocean surface emissivity (Meissner and Wentz 2012) with a statistical algorithm for hurricane-scale winds based on the NOAA Hurricane Research Division (HRD) Real-Time Hurricane Wind Analysis System (H*Wind; DiNapoli et al. 2012; Powell et al. 1998). We have confidence using WindSat for reliable high wind truth, as the physically based emissivity model used in WindSat processing is linear for wind speeds up to 40 m s^{-1} (Meissner and Wentz 2012).

The calibration target of the new QuikSCAT model function Ku-2011 is represented by these WindSat wind speeds developed at RSS. This paper begins with a description of the methodology used for developing Ku-2011 (section 2), presents an in-depth validation of the new Ku-2011 winds (section 3), discusses the impact of rain on the QuikSCAT wind vector retrievals (section 4), and illustrates the performance of the new Ku-2011 winds in sample tropical storms (section 5). A summary and a discussion of ongoing efforts toward a climate data record are presented in section 6.

2. The QuikSCAT Ku-2011 GMF

a. *QuikSCAT instrument*

The QuikSCAT mission objective has been to measure wind speed and direction over the global ocean in most weather conditions. QuikScat was in operation from July 1999 until November 2009. Its conical scanning pencil-beam antenna operated at 13.4 GHz (Ku band) with dual polarizations, each at a fixed Earth incidence angle of about 46° and 54° for horizontal polarization (H-pol) and vertical polarization (V-pol), respectively. Because of the scanning antenna, QuikSCAT had an unprecedented wide swath of about 1800 (1400) km at V-pol (H-pol), which covered about 90% of the earth in one day. Measurements along the swath are organized into 76 wind vector cells (WVC) at 25-km resolution, each including multiple backscatter observations made at both forward and aft looks.

Retrievals of ocean surface wind speed and direction are achieved with a semiempirical method by inverting a GMF for multiple scatterometer views within a WVC (Freilich and Dunbar 1993; Wentz and Smith 1999). More details about the QuikSCAT instrument, wind retrieval algorithm, and mission details are described in Freilich (1996), Hoffman and Leidner (2005), and Lungu and Callahan (2006).

b. *Derivation of the Ku-2011 GMF*

Since the original QuikSCAT Ku-2001 GMF was developed, more and higher-quality validation data at high wind speeds have become available. So, after the end of the operational use of QuikSCAT in 2009, when the instrument stopped rotating, we decided to develop a new GMF based on the 10 years of QuikSCAT backscatter measurements. The development of the new GMF Ku-2011 allowed us to correct some systematic biases at high winds and other minor issues, and to obtain wind retrievals consistent with those from radiometers [RSS version 7 (V7) data] in preparation for a wind climate data record.

The GMF is a transfer function that relates the radar backscatter cross section σ_0 to ocean surface wind speed and direction relative to the azimuthal look, and it depends on the radar beam incidence angle and radar signal polarization. QuikSCAT has an almost fixed incidence angle (with variations within 0.1°) for each polarization. Therefore, for each polarization, the σ_0 can be considered as dependent only on wind speed w and direction, and it can be easily expressed as a summation of harmonic functions of the wind direction φ_R relative to the looking angle (azimuth):

$$\sigma_0 = f(w, \varphi_R)_{\mathrm{pol}} \cong \sum_{i=0}^{N} A_i(w)_{\mathrm{pol}} \cos(i\varphi_R). \qquad (1)$$

The effect of neglecting the small incidence angle variability is on the order of 0.02–0.05 dB (for V-pol and H-pol), and would affect mostly very low winds (section 3b).

The coefficients $A_i(w)_{\mathrm{pol}}$ are empirically determined by matching a large number of σ_0 observations at all possible wind ranges to "true" observed surface winds. The new GMF Ku-2011 uses the RSS WindSat all-weather wind speed retrievals (http://www.remss.com/windsat) as calibration truth. The choice of WindSat as calibration was motivated by 1) the WindSat mission overlaps with several scatterometer missions and can be used as a common calibration for these; 2) WindSat has reliable winds at all wind speeds, particularly in the 20–30 m s^{-1} regime (Meissner and Wentz 2012); 3) WindSat can measure winds also in rainy and storm conditions; 4) WindSat also measures rain rate, useful for flagging rain-contaminated scatterometer retrievals; 5) WindSat hurricane winds had been validated versus HRD H*Wind; and 6) WindSat data provide 7 years (February 2003–November 2009) of global collocations with QuikSCAT, typically within 30–60 min of observation.

We developed the GMF Ku-2011 by collocating 7 years of QuikSCAT observed backscatter cross-section σ_0 with WindSat wind speeds, using a time window of 90 min (resulting in hundreds of millions collocations at all latitudes). Rain-contaminated data were excluded at this stage, as rain impacts the σ_0 and would bias the GMF if used. We used WindSat rain (Meissner and Wentz 2009; Meissner and Wentz 2006) to discard the σ_0 observations in the proximity of rain. To determine the harmonic coefficients $A_i(w)$, we binned all the QuikSCAT–WindSat collocations in a two-dimensional histogram with 0.2 m s^{-1} bins in wind speed and 2° in relative wind direction. For each wind speed bin, we calculated the harmonic coefficients $A_i(w)$ for a decomposition truncated at $N = 5$.

The choice of ground truth for wind speed and the use of a large number of available collocations are very important factors in determining the coefficients. Figure 2 shows the binned σ_0 contour lines for two cases, when using buoy wind speeds and when using WindSat winds. These lines display which wind speeds and directions are associated with a particular value of observed σ_0. At wind speeds below 15 m s^{-1}, using either buoys or WindSat for training the GMF does not have significant impact. Large differences between the two cases exist for winds above 15 m s^{-1}, for which there is a very limited number of buoy observations. As a result, the binned σ_0 lines using buoy data are very noisy, and if they were used in deriving a GMF would result in noisy and underestimated A_i coefficients. At lower winds the buoys and WindSat binned σ_0 overlap; therefore, we are confident we can use WindSat winds as a calibration truth at all wind speeds, rather than only for high winds. An alternative could have been to use buoys as ground truth for winds lower than 15 m s^{-1} and WindSat for higher winds. However, merging GMF A_i coefficients derived from different datasets has the disadvantage of resulting in a small spurious bump in the probability distribution function (PDF) for wind speed at the transition between the two wind regimes. The other advantage of not using buoys for the derivation of the GMF is that they can be used as an independent validation datasets for the scatterometer wind retrievals.

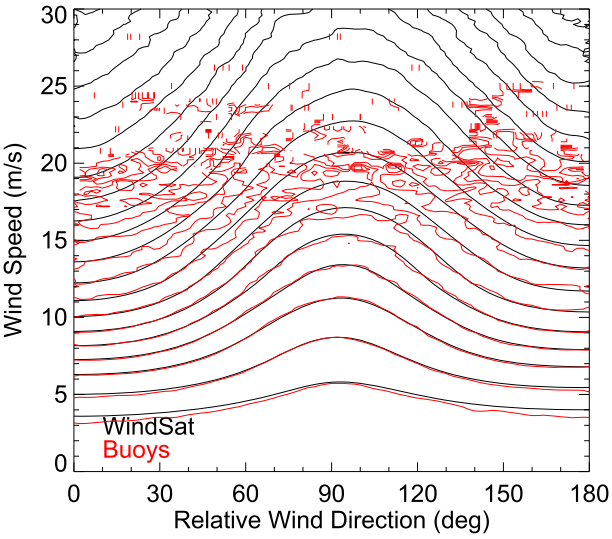

FIG. 2. Contour levels of the QuikSCAT observed backscatter histograms binned using collocated wind speeds from either WindSat (black) or buoys (red). This figure uses 7 years of V-pol QuikSCAT measurements (2003–09). CCMP is used for binning wind direction. The relative wind direction is limited to 0°–180° because of symmetry around zero.

WindSat wind directions are not sufficiently accurate at low winds for use as calibration truth (see Fig. 10). Instead, we used wind directions from the cross-calibrated

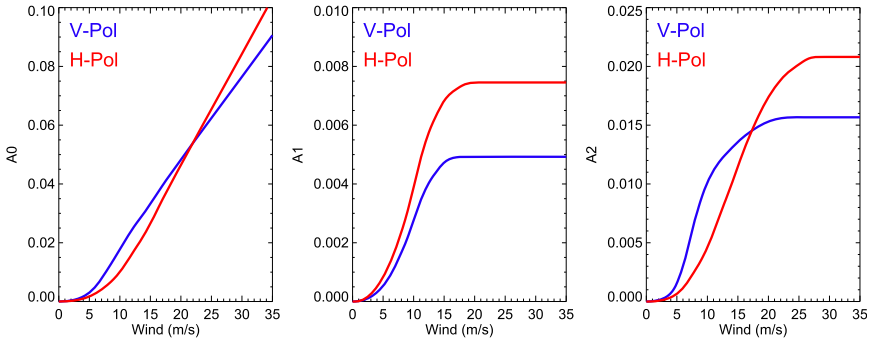

FIG. 3. Ku-2011 GMF (left) A_0, (middle) A_1, (right) A_2 coefficients for V-pol (blue) and H-pol (red), as a function of wind speed. Coefficient units are nondimensional.

multiplatform (CCMP) dataset (Atlas et al. 2008, 2011). The CCMP is a global 6-hourly satellite-derived wind dataset produced using a four-dimensional variational data assimilation (4DVAR) method of radiometer wind speeds, scatterometer wind ambiguities, conventional surface wind data, and winds from European Centre for Medium-Range Weather Forecasts (ECMWF) analyses and reanalyses as prior information. This product has a 0.25° resolution, and the CCMP wind directions are derived numerically using the ECMWF fields and rain-free QuikSCAT as input to the 4DVAR assimilation model. We also examined whether NCEP wind directions could be used instead of CCMP for training our GMF and got very similar results. Uncertainty in wind direction ground truth can impact the harmonic expansion coefficients $A_i(w)$ at low wind speeds. Therefore, we applied a correction to these coefficients to account for a spurious bias on the coefficients due to uncertainty in the wind direction from CCMP. The correction was estimated using a histogram method similar to the one described in Wentz and Smith (1999) but was determined using 9 years of σ_0 differences collocated with CCMP wind directions, uniformly distributed at all wind directions. The correction is most relevant at low winds and is negligible at high winds.

The coefficients $A_i(w)$ for the final GMF Ku-2011 were calculated in two steps. First, we performed a simple harmonic decomposition of the observed σ_0 binned using WindSat wind speed and CCMP wind direction, for every wind speed bin. The correction to compensate for the CCMP wind direction uncertainty is applied to these $A_i(w)$ coefficients. After this first step, some fine-tuning was necessary to adjust the coefficients at very high winds (above 25 m s^{-1}), where the number of σ_0 collocations is low, and at very low winds (below 5 m s^{-1}), where the correction based on the histogram method is not accurate. This was done because the noise in the retrievals (both of σ_0 and of the calibration wind speed and direction) at these wind regimes has the effect of artificially altering the coefficients of the harmonic analysis of the binned σ_0. The fine-tuning mostly involved the directional coefficients $A_1(w)$ and $A_2(w)$, and it was based on validation studies involving several years of the new QuikSCAT wind retrievals compared to buoys, and other satellite retrievals (more information on this process in section 3).

Our fine-tuning phase focused on making sure that for regimes with a low number of collocations the following conditions are met: 1) the high wind speeds from the new QuikSCAT winds match tightly collocated WindSat winds up to about 35 m s^{-1}); 2) the histograms of QuikSCAT wind direction match NCEP, at all winds. This is a particularly challenging problem at low winds, because the nondirectional coefficients in the GMF are very small and are very sensitive to small errors due to noise; 3) there is no cross-track bias in QuikSCAT retrievals compared to other validation data, and the wind speed PDFs for different regions of the swath overlap, meaning that they do not depend on the WVC position along the swath; 4) the A_i coefficients smoothly go to zero when the wind speed approaches zero; and 5) the $A_i(w)$ coefficients are smooth at winds above 25 m s^{-1}. To reduce the noise due to the harmonic decomposition obtained from a low number of collocations at high winds, we extrapolate an optimal linear behavior for wind speeds above 25–30 m s^{-1}, which better match the estimates of the harmonic decomposition. We achieve this by assuming that the A_0 coefficient slope is constant, and that the directional coefficients saturate at high winds, as suggested by the actual observations.

The final Ku-2011 GMF coefficients for V-pol and H-pol are displayed in Fig. 3. These figures show that about 90% of the backscatter signal is due to the nondirectional coefficient A_0. The directional coefficients A_1 and A_2 are about one order of magnitude smaller, and the remaining A_3–A_5 coefficients contribute only minimally. One aspect of the determination of the

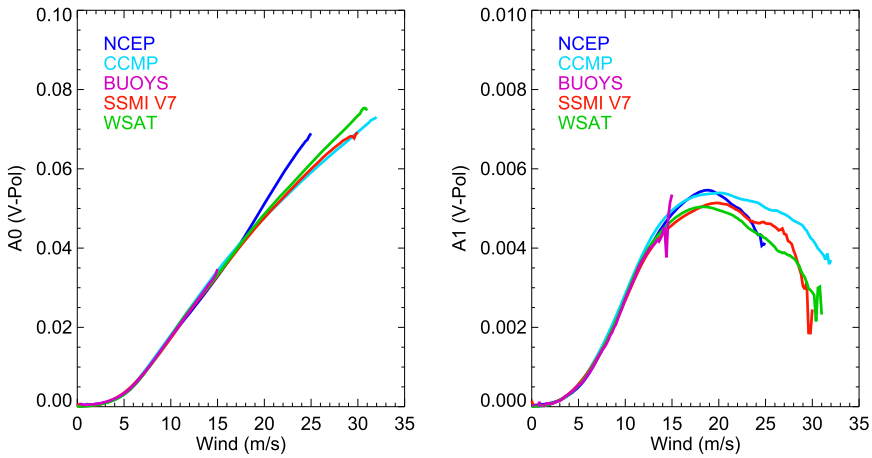

FIG. 4. The (left) A_0 and (right) A_1 V-Pol coefficients as determined from the harmonic decomposition of the binned observed σ_0, using different sources of ground truth for wind speed: NCEP, CCMP, buoys, SSM/I V7, and WindSat.

coefficients is how sensitive they are to the choice of our ground truth at high winds. In Fig. 4 we show the A_0 and A_1 V-pol coefficients determined using different datasets for calibration, without applying the fine-tuning described above: NCEP, buoy, SSM/I, CCMP, and WindSat. There are noticeable differences for wind speeds above $20\,\mathrm{m\,s^{-1}}$, where NCEP underestimates the wind speeds and results in significantly overestimated A_0 coefficients. For buoys, the very limited number of collocations above $13\,\mathrm{m\,s^{-1}}$ results in noisy and underestimated directional coefficients (A_1 in Fig. 4, magenta line). Figure 4 highlights the sensitivity of the GMF coefficients to the calibration wind speed used for the derivation. Errors in specifying the wind speed can be systematic and can result in constant high/low biases at different wind regimes for different calibration datasets. On the other hand, errors in the wind directions tend to be more random in nature and have less effect on the GMF calibration.

In April 2011, we reprocessed the complete QuikSCAT dataset (1999–2009) using the new GMF Ku-2011 (Ricciardulli and Wentz 2011). The reprocessed wind vector retrievals (version 4) were released to the public on the Remote Sensing Systems website (www.remss.com), where users can find swath data (L2B) and gridded 0.25° daily maps (L3), for ascending and descending passes. Also available on the website are composite maps for 3-day, weekly, and monthly averages, a description of all data products, and support code to read the data. The Ku-2011 GMF was delivered to JPL and is used to make their recently reprocessed QuikSCAT V3 12.5-km winds (Fore et al. 2013; available online at http://podaac.jpl.nasa.gov/dataset/QSCAT_LEVEL_2B_OWV_COMP_12).

3. Validation of the Ku-2011 QuikSCAT winds

a. Wind validation database

The validation database we use covers the entire QuikSCAT mission (1999–2009) and includes the following:

- In situ measurements from more than 200 global buoys from the U.S. National Data Buoy Center (NDBC; Gilhousen 1987), the Tropical Atmospheric Ocean (TAO)/TRITON array (McPhaden et al. 1998; PMEL 2013), the Prediction and Research Moored Array in the Tropical Atlantic (PIRATA; Bourlès et al. 2008), the Indian Ocean Research Moored Array for African–Asian–Australian Monsoon Analysis (RAMA; McPhaden et al. 2009), and the Canadian Marine Environmental Data Service (MEDS) coastal buoys of Canada (Gower 2002).
- Satellite winds (L2 and daily L3) from the radiometers SSM/I, TMI, WindSat V7 (Wentz 2013), distributed online (at www.remss.com).
- Model and data assimilation winds: the NCEP Global Data Assimilation System (GDAS) 6-hourly wind fields, at 1° resolution, and the CCMP 6-hourly wind fields, at 0.25° resolution (Atlas et al. 2008, 2011).
- Aircraft observations from the Greenland Flow Distortion Experiment (GFDex) off the tip of Greenland (Renfrew et al. 2009).
- Winds in storms from the NOAA HRD H*Wind analyses (DiNapoli et al. 2012; Powell et al. 1998, 2010; www.aoml.noaa.gov/hrd/index.html).

Most of the validation analyses reported here come from comparing 5 years (2003–07) of rain-free QuikSCAT winds (swath data) to each of the validation datasets

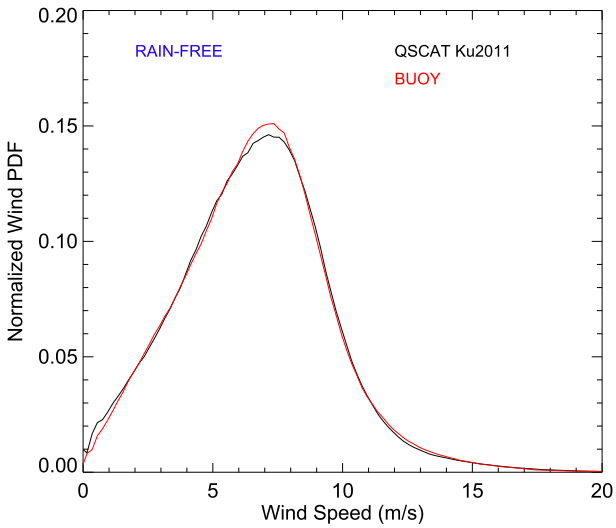

FIG. 5. Wind speed PDF for buoy winds (red) compared to the Ku-2011 QuikSCAT winds (black). The PDF statistics are based on 5 years of rain-free QuikSCAT winds collocated with winds from 200 quality-controlled global moored buoys within 50 km and a time window of 60 min.

listed above, within a 30–90-min time window. We remove rain-contaminated winds by using both the QuikSCAT rain flag and the collocated radiometer rain flag. Both rain flags are available within the RSS QuikSCAT 2LB (swath) and L3 (daily averaged) files.

b. *Validation of wind speed*

We compare the wind speed PDF of 5 years of rain-free QuikSCAT winds with the PDF built from buoys measurements collocated within 60 min and within a radius of 50 km from the QuikSCAT retrieval. Figure 5 illustrates that the two PDFs are in very good agreement at all wind speeds. Most of the changes in the new QuikSCAT winds are at high wind speeds and are therefore visible in comparisons to other validation winds. Figure 6 shows the joint PDFs versus buoys, NCEP GDAS, WindSat, CCMP, and SSM/I V7 winds. These PDFs contain 5 years of wind retrievals where WindSat and SSM/I are collocated within 90 min, buoys within 60 min, and the NCEP and CCMP 6-hourly data are interpolated linearly in space and time to match the QuikSCAT measurements. Figure 6 also displays the average bias between the pairs of datasets being compared (dashed line) and the standard deviation around the mean difference (error bars) as a function of wind speed. QuikSCAT and WindSat match very well at all wind speeds by design, without any bias and with an average standard deviation of 0.67 m s^{-1}. For all data, the standard deviation about the mean bias increases with wind speed, reaching 2–3 m s^{-1} in the 20–30 m s^{-1} wind regime, which is within the mission requirements at high winds (Lungu and Callahan 2006). The new QuikSCAT retrievals also compare very well at all wind speeds with the CCMP winds, which are mainly derived by assimilating satellite radiometer wind speeds (SSM/I V6, AMSR-E, TMI V4, and WindSat), and wind vector ambiguities from Ku-2001 QuikSCAT, and using numerically derived wind vectors from ECMWF operational analyses and reanalyses as background (Atlas et al. 2011). The joint PDFs for NCEP and buoy winds show that the QuikSCAT winds greater than 15 m s^{-1} are higher. Both buoys and NCEP winds are known to underestimate high winds. This was the main reason for not using either buoy or NCEP data to calibrate the new QuikSCAT GMF Ku-2011. Finally, the last panel in Fig. 6 shows that the QuikSCAT winds align very well with those from the SSM/I radiometers.

Figure 7 shows the differences between wind speeds obtained using the new QuikSCAT GMF, Ku-2011, and the previous version, Ku-2001. Other than the GMF, no other changes were made in the wind retrieval algorithm. The bias between the two QuikSCAT versions is illustrated as a function of CCMP and is apparent for winds greater than 15 m s^{-1}, where Ku-2001 data have been shown to be about 15%–20% too high (Fig. 12).

For a good-quality GMF, the wind speed validation statistics have to be independent of the swath location. Figure 8 shows the QuikSCAT–buoy wind speed difference as a function of the WVC position, numbered 1–76, from the left to the right side of the QuikSCAT swath. There is only a very small difference at the edges of the scan, where only retrievals from the V-pol channel exist. The H-pol swath is narrower. For studies requiring very high accuracy, users of the QuikSCAT swath (L2B) files should discard these swath edge winds.

Another important verification of the QuikSCAT winds is to look for regional biases, at any wind regime. Figure 9 shows the global bias map of rain-free QuikSCAT winds compared to NCEP (left) and WindSat (right). There are a few regions where small biases exist for NCEP, mostly in areas of strong spatial wind variability. These biases are caused by the diminished ability of the NCEP model to display small-scale motions, due to the model resolution (100 km) and the smoothing applied to the model wind field. When QuikSCAT is compared to WindSat, these bias regions are not present. However, there are significant biases in the meridional wind component. This could possibly be due to the lower skill of WindSat in retrieving wind direction with the current algorithm used for WindSat processing, which is based on one look only. A new algorithm using two looks (fore and aft) for much improved WindSat wind direction skill is under development (Wentz et al. 2014). While

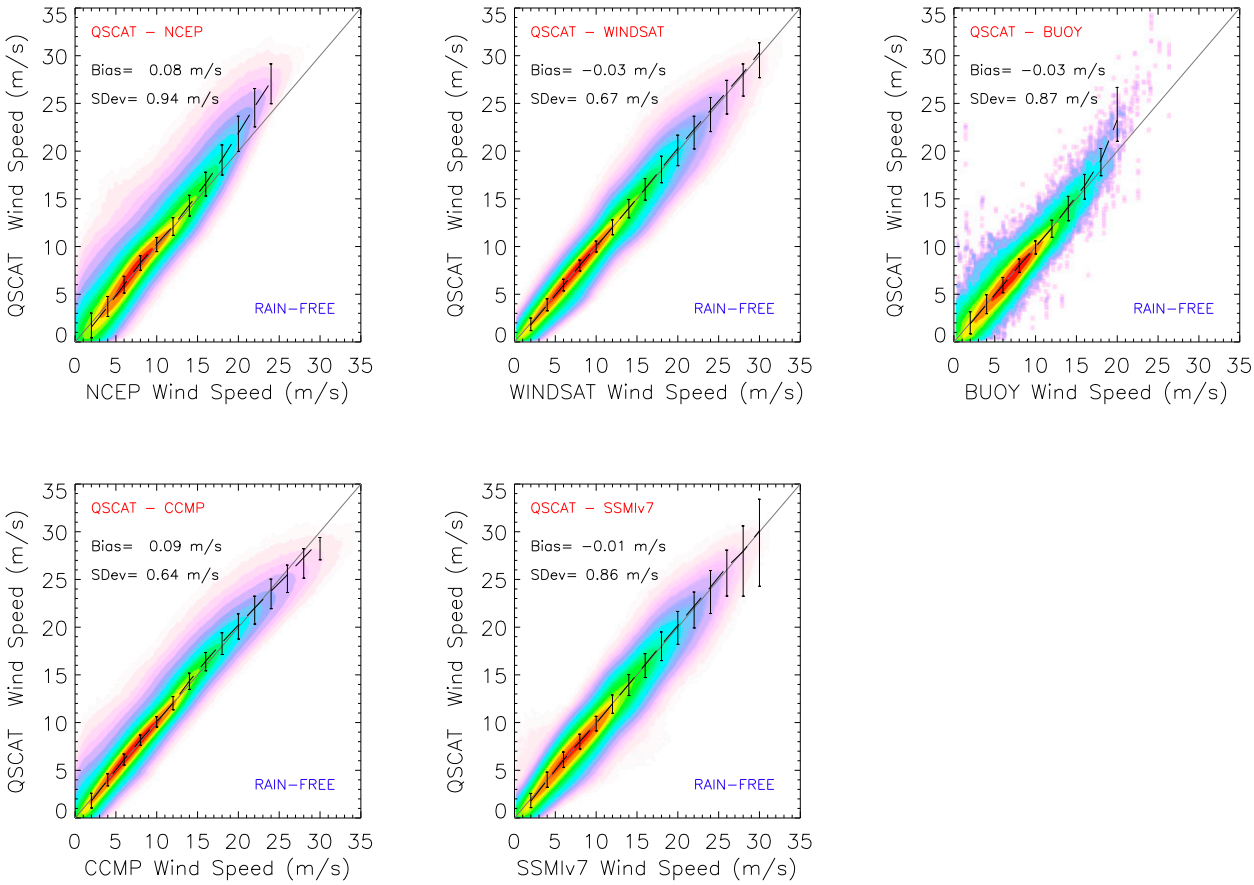

FIG. 6. Joint PDF for rain-free QuikSCAT Ku-2011 winds vs various validation data: NCEP GDAS, WindSat, buoys, CCMP, WindSat, and SSMI V7. Each validation dataset has been individually collocated with or interpolated to the QuikSCAT time of observation. The PDFs are normalized for better visualization. The thick dashed black lines represent the relative bias between the two wind datasets. The thin vertical lines represent the standard deviation about the average bias at selected wind speeds ($m\,s^{-1}$).

WindSat does not represent an independent validation of the QuikSCAT retrievals, as it was used to calibrate the Ku-2011 GMF, it is important to keep in mind that the calibration was done at a global scale. It is still a valuable exercise to compare QuikSCAT and WindSat biases at regional scales. NCEP winds are biased low compared to QuikSCAT winds in the southern extratropical oceans. Analysis of the bias stratified for different wind regimes (not shown) attributes this regional bias to the NCEP model underestimating the high winds.

The effect of neglecting the incidence angle variations (maximum 0.1°) in the GMF were studied by using the NSCAT GMF: they translated into an error of about 0.02–0.05 dB. While this is generally negligible, it might have some small impact for observations at very low winds (below $3\,m\,s^{-1}$), or some very small spurious trends if the QuikSCAT average incidence angle drifted in time. Future reprocessing of the QuikSCAT for the final climate data record will include the incidence angle dependency in the GMF, as recently done for the RapidScat GMF.

c. *Validation of wind direction*

To validate QuikSCAT wind direction, we use NCEP GDAS 6-hourly data, interpolated to the time and location of the rain-free QuikSCAT observations. Figure 10 shows the root-mean-square (RMS) difference of the QuikSCAT minus NCEP wind directions for the selected ambiguity, as a function of wind speed. For winds greater than $8\,m\,s^{-1}$ and up to $30\,m\,s^{-1}$, the uncertainty in the Ku-2011 wind direction is about 10°, much lower than the mission requirement of 20° in the 3–$30\,m\,s^{-1}$ range; (Lungu and Callahan 2006). There has been a significant improvement in the RMS for winds higher than $15\,m\,s^{-1}$ over the previous Ku-2001 QuikSCAT winds. This is the result of more accurate directional coefficients A_1 and A_2 in Ku-2011. The wind direction RMS increases at low winds, with values as high as 30° at $2\,m\,s^{-1}$. This is due to the greatly decreased

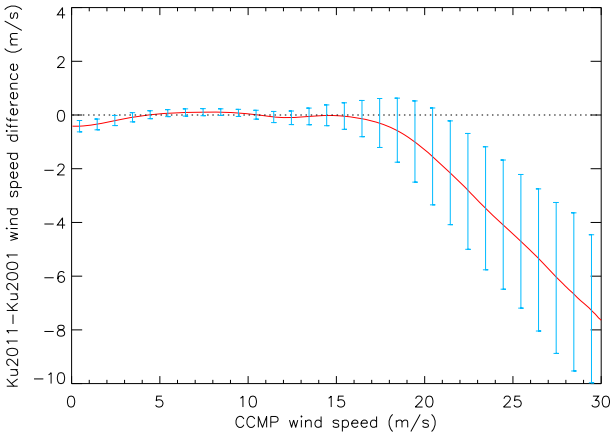

FIG. 7. Comparison of QuikSCAT Ku-2011 minus Ku-2001 wind speed (red line), as a function of CCMP wind speed. The blue error bars represent the standard deviation about the Ku-2011–Ku-2001wind speed difference.

sensitivity of the backscatter signal to the wind direction at low winds. Figure 10 also illustrates the wind direction RMS for WindSat winds as compared to NCEP. Because of the nature of the polarimetric wind direction signal in the surface emission (Meissner and Wentz 2002, 2012), WindSat has a lower sensitivity to wind direction compared to QuikSCAT, especially at winds below 6 m s^{-1}.

A more in-depth validation of the wind direction is achieved by analyzing the wind direction distribution relative to the satellite flight direction, a visualization method introduced by Ebuchi (1999, 2000). In this type of analysis, the frequency distribution of the observed wind direction is separated by ascending and descending passes and is shown as relative to the satellite flight direction in polar coordinates. When collecting data at a global scale, an anisotropic distribution should be expected due to the prevailing zonal direction of the winds (easterlies and westerlies), which are almost perpendicular to the direction of the satellite track. However, any other preferred wind retrieval direction that shows up in the plots is likely spurious and should be regarded as the result of either imperfections in the GMF, contamination due to rain signal, which tends to shift the wind directions cross track (Hilburn et al. 2006), or imperfections in the retrieval algorithm. In Fig. 11 the Ebuchi plots of rain-free QuikSCAT wind directions (for both Ku-2001 and Ku-2011) for the descending passes and for low (2–4 m s^{-1}), moderate (6–8 m s^{-1}) and high winds (20–22 m s^{-1}) are shown. The figure shows that QuikSCAT Ku-2001 had excellent skill in wind directions at moderate winds but was deficient at high winds. The Ku-2011 winds match the NCEP wind directions very well at all wind speeds.

In addition to validation studies, the Ebuchi diagrams can be used to fine-tune the GMF during the development phase. As mentioned in section 2, estimating the coefficients $A_i(w)$ directly from the harmonic decomposition of the binned σ_0 can lead to large errors at very low winds. This happens for more than one reason. The uncertainty in the calibration wind directions at low winds tends to smooth out the σ_0 curves as a function of relative wind direction and results in underestimated harmonic coefficients. The correction to the coefficients based on the histogram method has a low signal-to-noise ratio at winds below 5 m s^{-1} and is less reliable. Moreover, the number of σ_0 collocations with WindSat winds decreases dramatically at both low and high winds. This results in noisy σ_0 curves. For these reasons, we

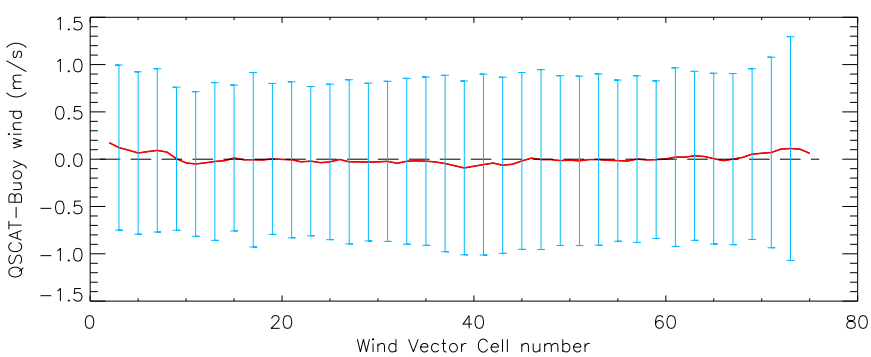

FIG. 8. QuikSCAT minus buoy wind speed differences (m s^{-1}), averaged overall wind speeds, as a function of the position along the satellite swath. There are 76 WVCs in a QuikSCAT swath. The WVC positions range from 1 (left edge of the swath) to 76 (right edge). The cyan error bars represent the standard deviation about the difference. Note that the standard deviation does not depend on the WVC position, except for the WVCs at the extreme edges of the scan, where the retrieval quality is slightly degraded due to only V-pol measurements contributing to these wind retrievals.

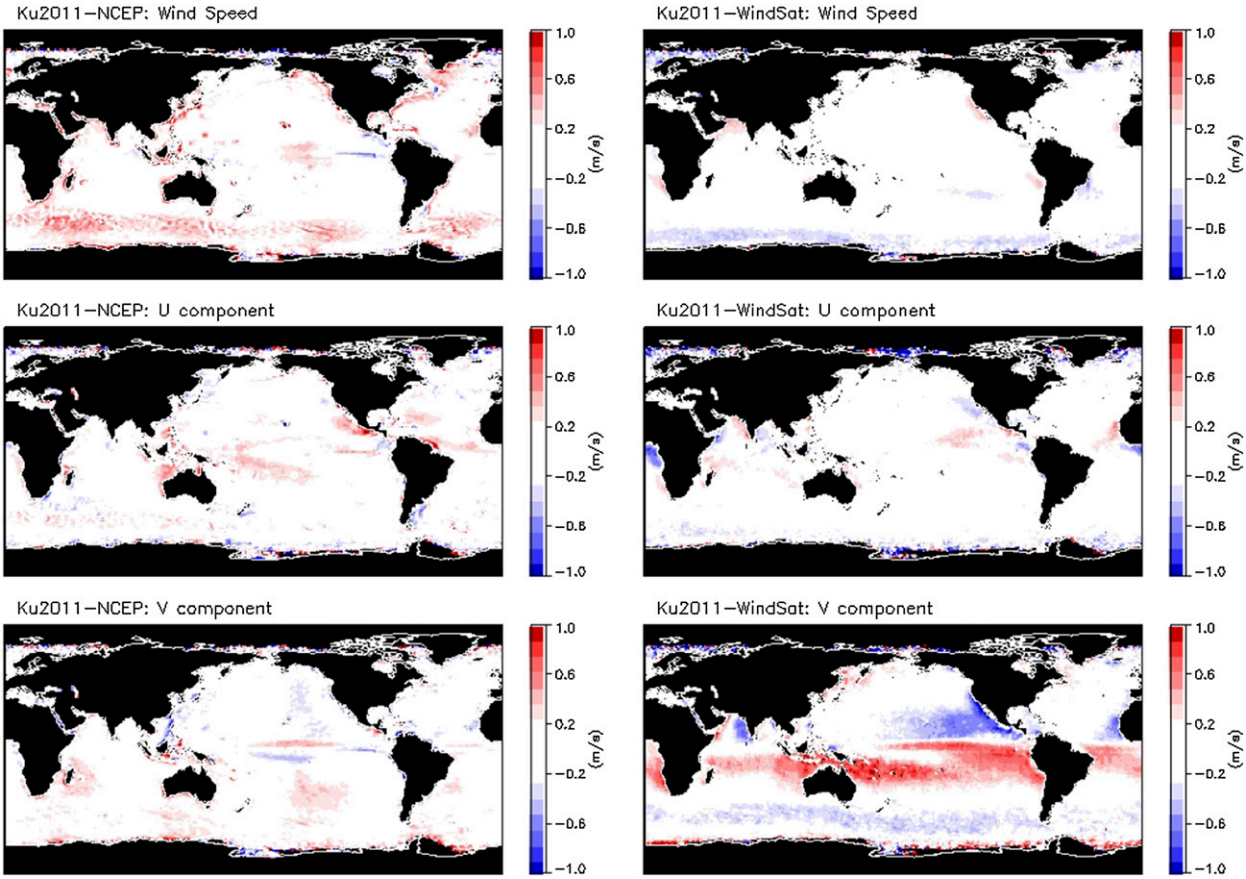

FIG. 9. Global maps for rain-free QuikSCAT vs (left) NCEP or (right) WindSat. The bias is displayed for the (top) wind speed, and the (middle) zonal and (bottom) meridional wind components.

empirically fine-tuned the A_1 and A_2 directional coefficients for winds below $5\,\mathrm{m\,s^{-1}}$ by analyzing the Ebuchi diagrams. The Ebuchi diagram at very low winds for the old Ku-2001 wind directions have a tendency of displaying two spurious perpendicular lobes. We corrected this artificial directional anisotropy by lowering A_1 and A_2 in Ku-2011.

d. Aircraft validation of high wind speeds

Our goal for the GMF Ku-2011 was to improve retrievals at high wind speeds. It is important to use an independent dataset with sufficient high winds to validate both the GMF and the WindSat winds used for calibration. We use aircraft wind measurements made during GFDex off the tip of Greenland (Renfrew et al. 2009). Because of the extratropical location of these measurements, they are mostly free of rain and well represent the high winds in this region. One hundred and fifty measurements were made by an aircraft-mounted turbulent probe during five aircraft missions. These measurements were converted to an equivalent neutral wind at a height of 10 m. The maximum wind speed observed during flights for which collocated QuikSCAT winds are available is $25\,\mathrm{m\,s^{-1}}$. Figure 12 shows that the Ku-2011 QuikSCAT winds match very well with the aircraft winds, both for wind speed and wind direction. Figure 12 also shows Ku-2001 QuikSCAT and WindSat wind comparisons. In addition to a significant reduction of the wind speed bias, Fig. 12 illustrates a clear improvement of QuikSCAT Ku-2011 wind direction at high winds (RMS = 9°) over the Ku-2001 (RMS = 15°), represented by the direction RMS difference with aircraft measurements. This is due to the improved nondirectional coefficients at high winds in the new Ku-2011 GMF. WindSat retrievals at high winds show a remarkable similarity with the slope in wind speed of the aircraft measurements, with just a little bias in wind speed and good wind direction retrieval skill (RMS = 12°). In the future, we plan more high wind speed validation when additional reliable measurements become available (i.e., with high-resolution rain-free aircraft measurements in tropical and extratropical storms, or dropsondes).

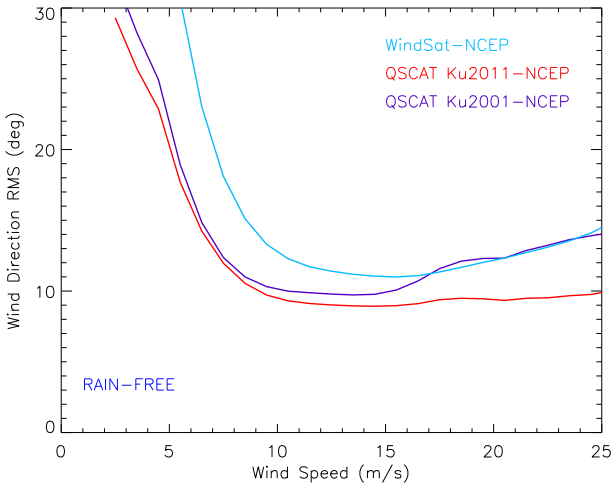

FIG. 10. Wind direction RMS difference for QuikSCAT minus NCEP winds as a function of wind speed, for Ku-2011 (red) or Ku-2001 (purple), or WindSat (one-look algorithm) minus NCEP winds (teal). The statistics are based on 5 years of QuikSCAT or WindSat data.

An alternative indirect way to validate the QuikSCAT Ku-2011 and WindSat high wind speeds is to compare the statistics of the hurricane-force extratropical cyclones from QuikSCAT versus data from the extensive database developed at the NOAA Ocean Prediction Center from aircraft using a Stepped Frequency Microwave Radiometer (SFMR) flying into cyclones (Uhlhorn et al. 2007). So far, preliminary studies (Jelenak et al. 2013) showed a very good performance of Ku-2011 in extratropical cyclones. More efforts are currently under way.

4. Rain impact on QuikSCAT retrievals

The main mechanisms affecting backscatter observations in rain are 1) atmospheric attenuation of the direct and backscattered microwave signal (resulting in a negative wind speed bias), 2) backscattering of the direct signal from the raindrops (positive bias), and 3) a "splash" effect of the raindrops that alters the ocean surface roughness (either positive or negative bias). These rain effects are difficult to model and cannot be easily removed from the scatterometer measurements. Therefore, in the development of the GMF, we chose to discard potentially rain-contaminated backscatter measurements, using collocated rain estimates made by the SSM/I and WindSat radiometers. As a result, the Ku-2011 GMF was specifically designed for rain-free conditions. For this reason, wind vector observations in rain conditions might be biased. The typical effect of rain is a positive bias at low winds (where rain backscatter effect dominates) and a negative bias at high winds (due to rain attenuation).

To estimate the impact of rain on the QuikSCAT retrievals, we collected 5 years of QuikSCAT winds and collocated radiometer rain rates, and stratified the winds as a function of the observed rain rate. Figure 13 shows the QuikSCAT wind speed bias versus WindSat, as a function of rain rate. By design, rain-free QuikSCAT retrievals (dashed line) are consistent with WindSat. For QuikSCAT wind retrievals in rain, the bias is clearly proportional to the rain intensity and is very pronounced at low wind speeds. At low winds in heavy rain, the wind bias might be as high as $10\,\mathrm{m\,s^{-1}}$. Wind speeds between 15 and $25\,\mathrm{m\,s^{-1}}$ are less affected by rain, as the negative (attenuation) and positive (rain backscatter) effects balance out. It is interesting to look at the rain impact on the QuikSCAT Ku-2001 wind retrievals, also in Fig. 13. There is a mixed impact of rain at high winds, which is the result of two effects: 1) an incorrect GMF produces spurious positive biases, leading to overestimated high winds; and 2) for high rain rates, the attenuation effect of raindrops results in a negative bias at high winds. The two effects cancel each other for rain rates of about $6\,\mathrm{mm\,h^{-1}}$. For higher rain rates, the negative rain impact dominates.

Wind direction is also contaminated by the rain signal. Rain-contaminated wind directions have a tendency of being oriented in a direction perpendicular to the satellite track (Stiles and Yueh 2002; Tournadre and Quilfen 2003). In raining conditions, the ambiguity removal skill of the wind retrieval algorithm is severely affected. Some of these rain effects can be seen in the storms in Figs. 14, 15, presented in the next section.

Wind vector measurements are provided in the L2B (swath) files even during rain, as it might be beneficial not to have a data gap for some applications and instead have continuous observations of possibly lower quality. For applications that require high accuracy, we recommend not using winds in rain. To omit rain-affected data, we use the rain flags provided in the files. Obviously, this will result in a loss of data.

5. Wind retrievals in storms

Tropical cyclones are usually characterized by areas of very strong winds (greater than $18\,\mathrm{m\,s^{-1}}$) and intense rain. Because of the coexistence of wind and rain, QuikSCAT retrievals in tropical storms and hurricanes might be biased. Figure 14 shows an example of Hurricane Fabian on 4 September 2003. The first panel displays the wind field from NOAA HRD H*Wind. H*Wind is a numerical objective analysis that incorporates all measurements available during the storm (mostly from aircraft flying in hurricanes and land-based radars). H*Wind fields closest in time to the WindSat and QuikSCAT satellite overpasses are used in our

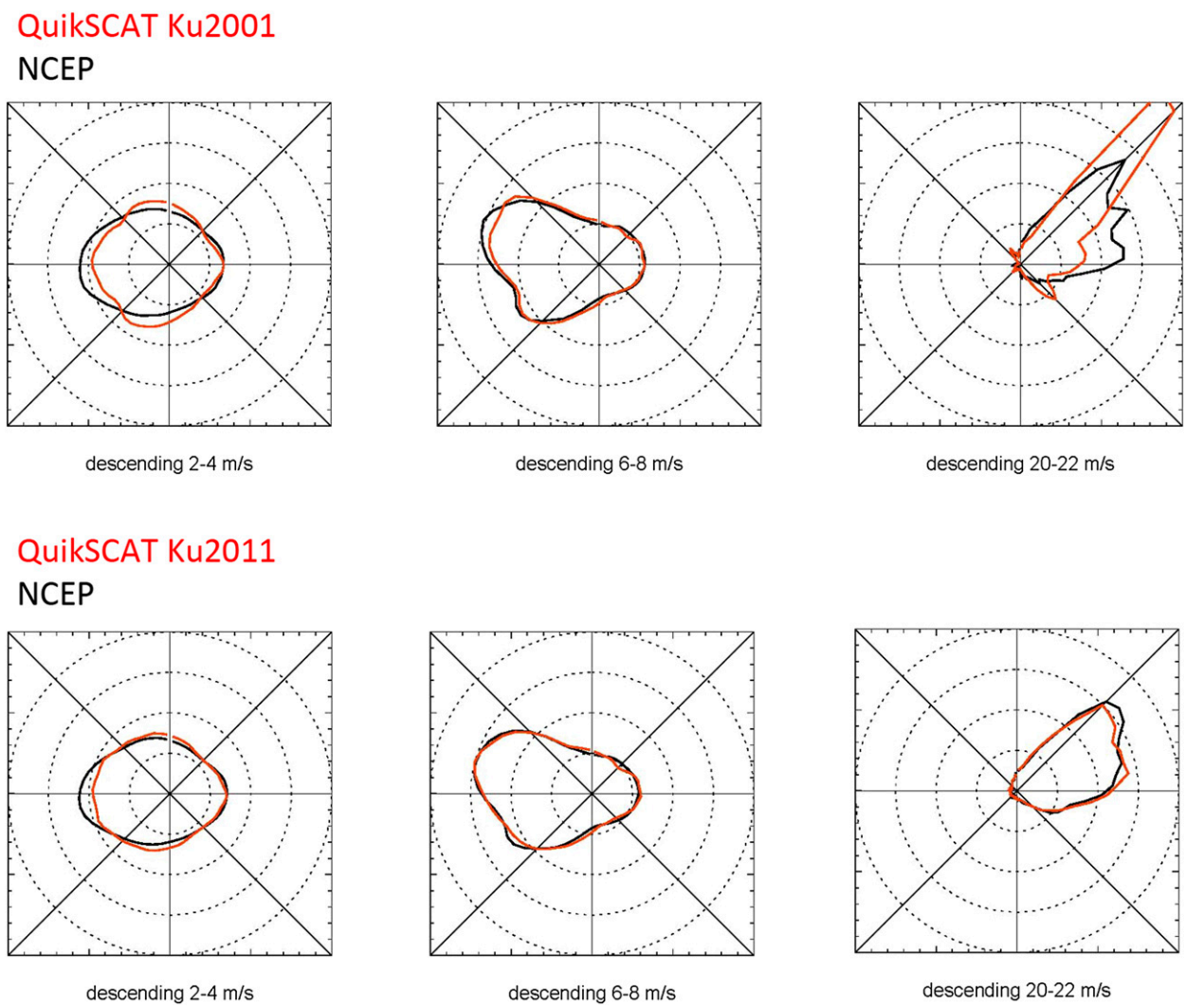

FIG. 11. Wind directional histograms (Ebuchi diagrams) for QuikSCAT (red line) vs NCEP (black line), for three wind regimes: (left) low (2–4 m s^{-1}), (middle) moderate (6–8 m s^{-1}), and (right) high winds (20–22 m s^{-1}). Displayed are retrievals for descending passes only. Retrievals with (top) QuikSCAT Ku-2001and (bottom) the new GMF Ku-2011. These diagrams were constructed using 5 years of data.

comparison. HRD winds are provided as 1-min sustained surface winds at a fine resolution of 5 km. We resampled them to the WindSat footprint sampling size (50 km) and scaled them to 10-min sustained winds (Meissner and Wentz 2009). As they are produced by a numerical analysis, HRD wind vectors are very smooth and their spatial structure is quite uniform and symmetric. The second and third panels from the left show the wind fields from the WindSat V7 all-weather algorithm and the QuikSCAT Ku-2011 winds, while the last panel shows the WindSat V7 rain rates. We see that the WindSat all-weather algorithm captures well the structure and intensity of the storm, although the wind direction is somewhat noisy. This is due to the small radiometer wind direction signal, which becomes strongly attenuated in rainy conditions. QuikSCAT wind vectors (third panel) are less noisy, as expected. The QuikSCAT maximum wind speeds for this storm (as well as for other analyzed storms, not shown) are consistent with HRD and WindSat winds. However, the structure of the storm is obviously affected by rain, especially in the northwest quadrant, where wind speeds are significantly underestimated. This rain impact on the QuikSCAT storm wind speeds is consistent with the results of our analysis described in section 4. QuikSCAT wind direction retrievals show good skill even in heavy rain. The scatterometer detects the eye of the storm but does not obtain the expected low wind speeds because of the positive rain bias at low wind speeds (see Fig. 13). The slight dislocation of the satellite view of the hurricane eye as compared

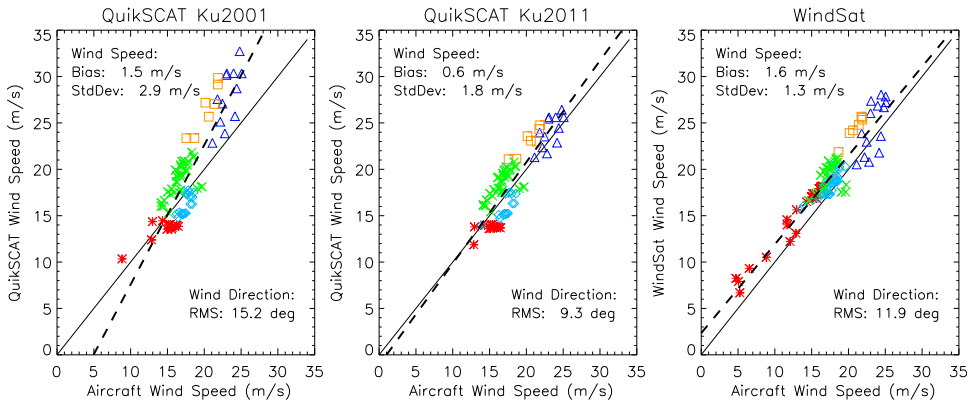

FIG. 12. Aircraft winds for GFDex compared to (left) QuikSCAT Ku-2001, (middle) QuikSCAT Ku-2011, and (right) WindSat winds. Each color refers to a different mission flight. The small wind speed bias and standard deviation compared to aircraft measurements, and the RMS difference in wind direction are listed in each plot. The WindSat comparison is from Meissner and Wentz (2012) and refers to the low-frequency channel with a resolution of about 35 km.

to the HRD wind field is likely due to the minor temporal mismatch between them.

Figure 15 illustrates another example, for Hurricane Katrina on 28 August 2005. The Ku-2011 GMF has lower overall wind speed and a more rotational flow, correcting the cross-track wind direction bias in Ku-2001 in the northwest quadrant of the storm. The QuikSCAT Ku-2011 retrievals are also more consistent than Ku-2001 with the wind field from the NCEP GDAS. Many other sample storms were examined and they displayed similar results to those discussed here.

6. Summary and conclusions

In this paper we have described the methodology for the development of a new series of scatterometer geophysical model functions that aims at making all the scatterometer winds consistent with each other and with the radiometer winds. Most of the difficulty of such an endeavor lies in the cross calibration of the wind speeds, as observed wind speeds are more susceptible to systematic errors. Wind direction errors are more random in nature, and it is unlikely they give raise to spurious biases in the wind time series composed using different sensors.

This represents a first milestone toward the development of a climate data record of ocean vector winds. The new GMF Ku-2011 was used to reprocess the QuikSCAT winds. We also presented a thorough validation of the new QuikSCAT wind speeds and wind directions. The QuikSCAT Ku-2011 winds are publicly available online (at www.remss.com), and the GMF is shared with

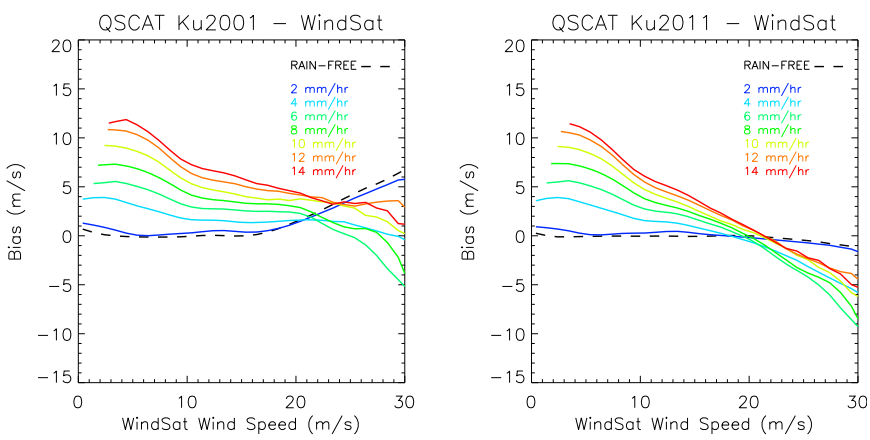

FIG. 13. QuikSCAT minus WindSat wind speeds, stratified according to WindSat rain rates, for (left) Ku-2001 and (right) Ku-2011. Each curve corresponds to a different rain-rate regime, from rain-free (black, dashed) to high rain (red). We used 5 years of QuikSCAT wind retrievals collocated within 90 min with WindSat.

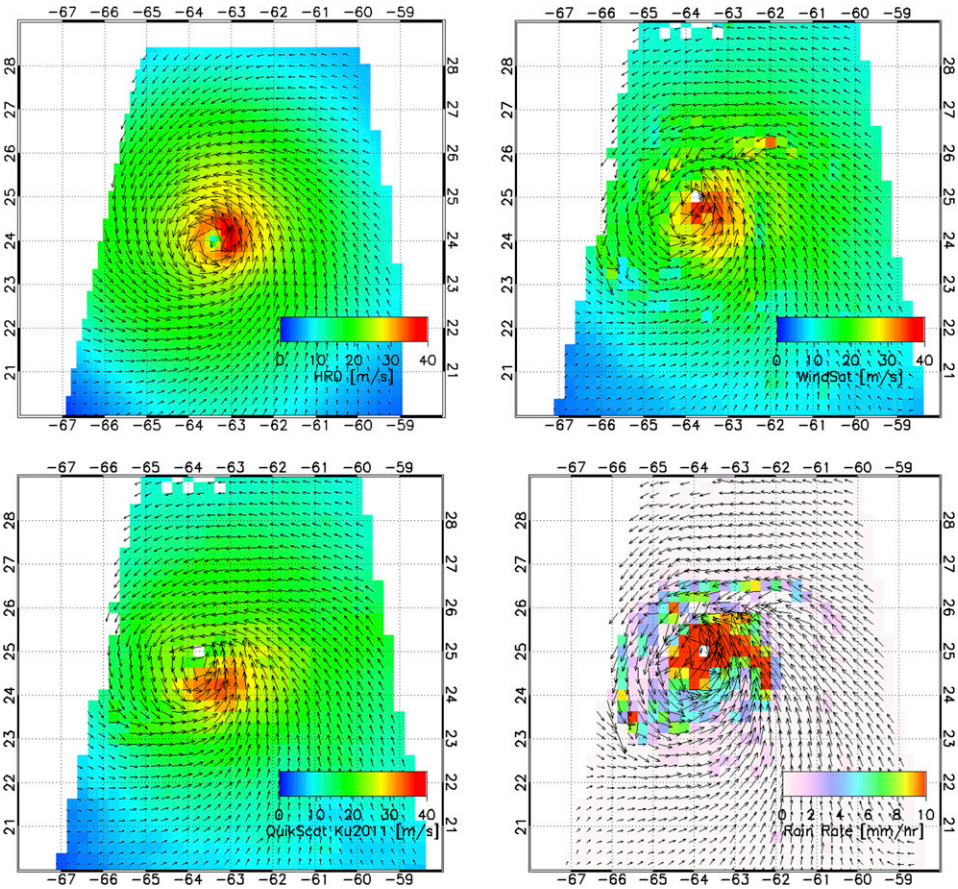

FIG. 14. Wind speed for Hurricane Fabian at 1030 UTC 4 Sep 2003. H*Winds from (top left) HRD, (top right) WindSat V7 all-weather winds, (bottom left) QuikSCAT Ku-2011 winds, and (bottom right) WindSat rain rates.

institutions that request it. The QuikSCAT Ku-2011 GMF was developed using the WindSat V7 rain-free winds as a calibration standard, as they are considered accurate up to 35 m s^{-1}, or even higher. The Ku-2011 winds display a great improvement in wind speed and direction for high winds compared to the previous GMF Ku-2001. The QuikSCAT wind retrievals are significantly affected by rain at low wind speeds, as expected. We advise users to flag these rain-contaminated data by using the rain flags provided in the files. At high wind speeds in storms, the impact of rain is less severe. In many cases, users might benefit more from using high-speed rain-affected winds rather than discarding them as rain contaminated.

Our long-term goal is to create satellite products with high accuracy that meet a demanding intercalibration standard, a necessary requirement for climate data records.

We recently reprocessed all our microwave radiometer datasets after a thorough intercalibration process. The RSS microwave radiometer data, version 7 (Wentz 2013), are already available online (at www.remss.com) for all the SSM/I, SSMIS, AMSR-E, AMSR2, TMI, and WindSat. The Ku-2011 RSS QuikSCAT can therefore be considered cross calibrated with all these radiometer winds. The JPL QuikSCAT V3 winds were also recently reprocessed with the Ku-2011 GMF. The JPL rain-free V3 winds (not shown) agree with the RSS QuikSCAT winds within 0.1 m s^{-1}, with an average bias (standard deviation) of about 0.04 m s^{-1} (0.45 m s^{-1}) despite the differences in processing algorithm and higher-resolution product. A slightly higher average bias is found at high winds (about 0.2 m s^{-1}).

The more than 20 years of scatterometer wind vectors provide great insight into the climate variability of surface wind patterns at a global scale. Integrating the scatterometers and radiometer ocean vector winds to create an intercalibrated climate data record with the accuracy required for climate research is a challenging goal. A necessary requirement when combining different datasets is to use a consistent methodology in the wind retrievals (National Research Council 2004). By using WindSat as a calibration ground truth, the new

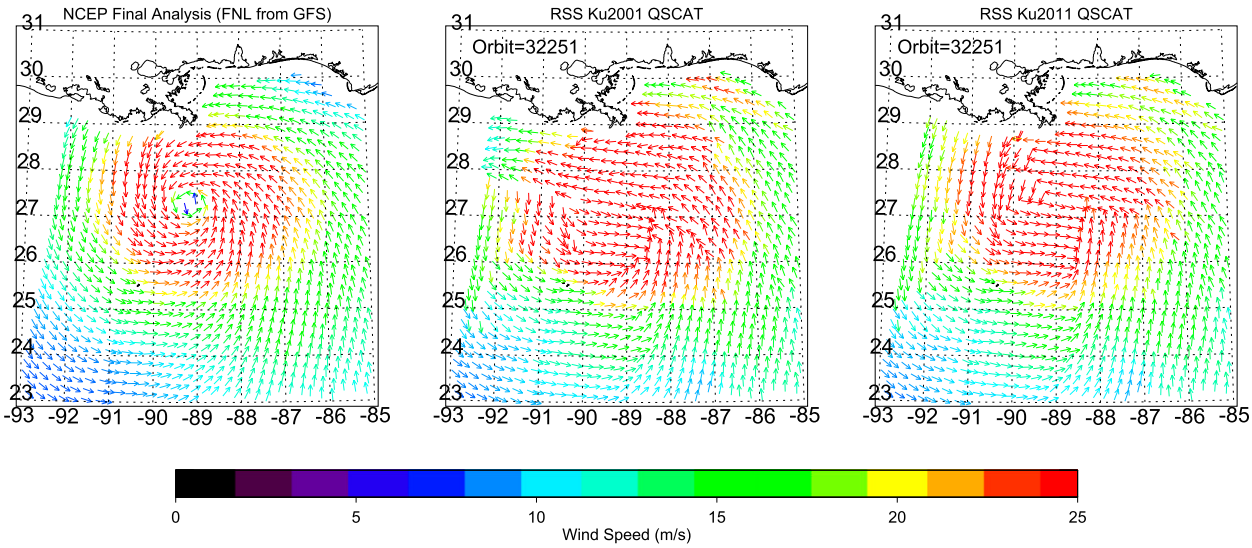

FIG. 15. Ocean surface winds for Hurricane Katrina from (left) NCEP GDAS, (middle) QuikSCAT retrievals with the Ku-2001 model function, and (right) Ku-2011 GMF. This case study refers to Katrina at 2353 UTC 28 Aug 2005 (QuikSCAT orbit 32251). All satellite winds are included, even those in rain.

QuikSCAT winds are now consistent with all the RSS V7 radiometer winds, and their accuracy is within the requirements for climate-quality data. To diagnose any drift or calibration error, we compared global monthly time series of QuikSCAT rain-free wind speeds with rain-free WindSat winds, SSM/I *F13* V7 winds, NCEP GDAS, and the CCMP winds (Fig. 16). There is an apparent small bias in 2008 between SSM/I *F13* and QuikSCAT that might be due to the loss of the 85-GHz channel in *F13* in 2008. A smaller bias in 2008 is present in QuikSCAT comparisons with NCEP and CCMP. The NCEP reanalyses and CCMP both assimilate QuikSCAT winds and SSM/I winds or radiances; therefore, the comparison does not resolve the source of the bias. As QuikSCAT compares well with WindSat for the same time period, we suspect the bias is due to SSM/I. Note that the SSM/I *F13* has a local time ascending node (LTAN) at about 1800 LT, which has been fairly constant during the duration of the mission. QuikSCAT LTAN is 0600 LT, with QuikSCAT ascending passes crossing with *F13* descending passes at the equator. WindSat LTAN is about the same as SSM/I *F13*. Therefore, the differences between QuikSCAT and SSM/I in 2008 cannot be attributed to drifting orbits or the effects of diurnal variability.

The most important conclusion of the comparison in Fig. 16 is the overall consistency of the satellite global monthly time series, within 0.1 m s^{-1}. This is the level of accuracy required for climate studies.

In addition to QuikSCAT, we are developing a series of wind vector datasets from other scatterometer missions (ASCAT-A and ASCAT-B, ERS, OSCAT, and the recent RapidScat) that will be processed in a manner consistent with QuikSCAT. We started with the European scatterometer ASCAT (Figa-Saldaña et al. 2002; Verspeek et al. 2010) on *Metop-A* and developed a new C-band GMF based on a methodology similar to the one described here for Ku-2011 (Ricciardulli and Wentz

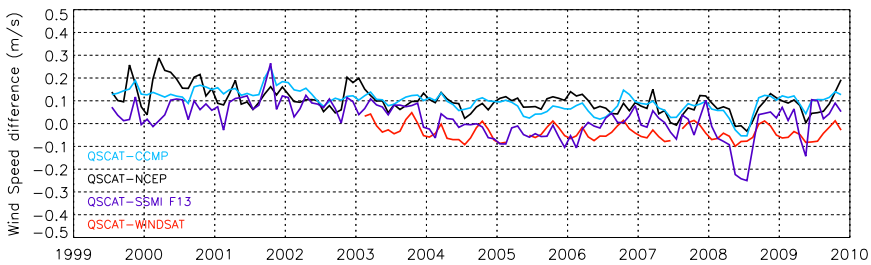

FIG. 16. Wind anomaly monthly time series difference between QuikSCAT and other collocated validation datasets: SSM/I *F13* (purple), WindSat (red), NCEP (black), and CCMP (cyan). WindSat retrievals used here refer to the lower channel (10 GHz).

2012, 2013). RSS ASCAT winds are publicly available online (www.remss.com). *ERS-1* winds (starting in 1991) will be processed using a modified version of our C-band GMF developed for ASCAT but will extended to lower incidence angles. Preliminary *Aquarius* L-band scatterometer winds consistent with the V7 radiometer winds have been produced (Meissner et al. 2014), and a similar methodology will be applied to produce L-band winds from the SMAP scatterometer.

When all these scatterometer data are processed in a consistent manner, we will have a 25-yr climate data record (CDR) of ocean vector winds. This CDR will be valuable for studying the decadal-scale variability of the ocean winds, and the related impact of the variability on air–sea interaction, ocean circulation, climate, and on the global water cycle. Even before all these data will be merged in a unique dataset, providing the users with cross-calibrated and consistently processed wind vector datasets for each sensor prevents or minimizes spurious biases when used for applications like building global datasets of analyzed winds (i.e., CCMP) or of surface fluxes (OAFlux, Yu and Weller 2007; SeaFlux, Roberts et al. 2010), for model comparisons or for climate studies using different sensors at different times (Robertson et al. 2014).

Acknowledgments. This research was supported by the NASA Ocean Vector Wind Science Team, NASA Contract NNH10CD55C. WindSat data are produced by Remote Sensing Systems (RSS) and are sponsored by the NASA Earth Science MEaSUREs DISCOVER Project and the NASA Earth Science Physical Oceanography Program. The authors thank Thomas Meissner (RSS) for the insight and discussions on WindSat data; and Deborah Smith (RSS), Kyle Hilburn (RSS), and three anonymous reviewers for their comments on the original manuscript.

REFERENCES

Atlas, R. M., and Coauthors, 2001: The effects of marine winds from scatterometer data on weather analysis and forecasting. *Bull. Amer. Meteor. Soc.*, **82**, 1965–1990, doi:10.1175/1520-0477(2001)082<1965:TEOMWF>2.3.CO;2.

——, R. N. Hoffman, J. Ardizzone, S. M. Leidner, and J.-C. Jusem, 2008: A new cross-calibrated, multi-satellite ocean surface wind product. *2008 IEEE International Geoscience and Remote Sensing Symposium: Proceedings*, Vol. 1, IEEE, I-106–I-109.

——, ——, ——, ——, J. C. Jusem, D. K. Smith, and D. Gombos, 2011: A cross-calibrated, multiplatform ocean surface wind velocity product for meteorological and oceanographic applications. *Bull. Amer. Meteor. Soc.*, **92**, 157–174, doi:10.1175/2010BAMS2946.1.

Bourassa, M. A., S. T. Gille, D. L. Jackson, J. B. Roberts, and G. A. Wick, 2010: Ocean winds and turbulent air-sea fluxes inferred from remote sensing. *Oceanography*, **23**, 36–51, doi:10.5670/oceanog.2010.04.

Bourlès, B., and Coauthors, 2008: The PIRATA program: History, accomplishments, and future directions. *Bull. Amer. Meteor. Soc.*, **89**, 1111–1125, doi:10.1175/2008BAMS2462.1.

Chelton, D. B., and S.-P. Xie, 2010: Coupled ocean-atmosphere interaction at oceanic mesoscales. *Oceanography*, **23**, 52–69, doi:10.5670/oceanog.2010.05.

——, and Coauthors, 2001: Observations of coupling between surface wind stress and sea surface temperature in the eastern tropical Pacific. *J. Climate*, **14**, 1479–1498, doi:10.1175/1520-0442(2001)014<1479:OOCBSW>2.0.CO;2.

DiNapoli, S. M., M. A. Bourassa, and M. D. Powell, 2012: Uncertainty and intercalibration analysis of H*Wind. *J. Atmos. Oceanic Technol.*, **29**, 822–833, doi:10.1175/JTECH-D-11-00165.1.

Draper, D. W., and D. G. Long, 2004a: Evaluating the effect of rain on SeaWinds scatterometer measurements. *J. Geophys. Res.*, **109**, C02005, doi:10.1029/2002JC001741.

——, and ——, 2004b: Simultaneous wind and rain retrieval using SeaWinds data. *IEEE Trans. Geosci. Remote Sens.*, **42**, 1411–1423, doi:10.1109/TGRS.2004.830169.

Ebuchi, N., 1999: Statistical distribution of wind speeds and directions globally observed by NSCAT. *J. Geophys. Res.*, **104**, 11 393–11 403, doi:10.1029/98JC02061.

——, 2000: Evaluation of NSCAT-2 wind vectors by using statistical distributions of wind speeds and directions. *J. Oceanogr.*, **56**, 161–172, doi:10.1023/A:1011183029009.

Entekhabi, D., and Coauthors, 2010: The Soil Moisture Active Passive (SMAP) mission. *Proc. IEEE*, **98**, 704–716, doi:10.1109/JPROC.2010.2043918.

Fernandez, D. E., J. R. Carswell, S. Frasier, P. S. Chang, P. G. Black, and F. D. Marks, 2006: Dual-polarized C- and Ku-band ocean backscatter response to hurricane-force winds. *J. Geophys. Res.*, **111**, C08013, doi:10.1029/2005JC003048.

Figa-Saldaña, J., J. J. W. Wilson, E. Attema, R. V. Gelsthorpe, M. R. Drinkwater, and A. Stoffelen, 2002: The advanced scatterometer (ASCAT) on the meteorological operational (MetOp) platform: A follow on for European wind scatterometers. *Can. J. Remote Sens.*, **28**, 404–412, doi:10.5589/m02-035.

Fore, A. G., B. W. Stiles, A. H. Chau, B. A. Williams, R. S. Dunbar, and E. Rodriguez, 2013: Point-wise wind retrieval and ambiguity removal improvements for the QuikSCAT climatological data set. *IEEE Trans. Geosci. Remote Sens.*, **52**, 51–59, doi:10.1109/TGRS.2012.2235843.

Freilich, M. H., 1996: SeaWinds algorithm theoretical basis document. NASA Doc. ATBD-SWS-01, 56 pp.

——, and R. S. Dunbar, 1993: A preliminary C-band scatterometer model function for the ERS-1 AMI instrument. *Proceedings of First ERS-1 Symposium on Space at the Service of Our Environment*, Vol. 1, ESA Publ. SP-359, 79–83.

——, and B. A. Vanhoff, 1999: QuikSCAT vector wind accuracy: Initial estimates. *Proc. QuikSCAT Cal/Val Early Science Meeting*, Pasadena, CA, JPL.

Gaiser, P. W., and Coauthors, 2004: The WindSat spaceborne polarimetric microwave radiometer: Sensor description and early orbit performance. *IEEE Trans. Geosci. Remote Sens.*, **42**, 2347–2361, doi:10.1109/TGRS.2004.836867.

Gilhousen, D. B., 1987: A field evaluation of NDBC moored buoy winds. *J. Atmos. Oceanic Technol.*, **4**, 94–104, doi:10.1175/1520-0426(1987)004<0094:AFEONM>2.0.CO;2.

Gower, J. F. R., 2002: Temperature, wind and wave climatologies, and trends from marine meteorological buoys in the

northeast Pacific. *J. Climate*, **15**, 3709–3718, doi:10.1175/1520-0442(2002)015<3709:TWAWCA>2.0.CO;2.

Hilburn, K. A., F. J. Wentz, D. K. Smith, and P. D. Ashcroft, 2006: Correcting active scatterometer data for the effects of rain using passive microwave data. *J. Appl. Meteor. Climatol.*, **45**, 382–398, doi:10.1175/JAM2357.1.

Hoffman, R. N., and S. M. Leidner, 2005: An introduction to the near-real-time QuikSCAT data. *Wea. Forecasting*, **20**, 476–493, doi:10.1175/WAF841.1.

Isaksen, L., and A. Stoffelen, 2000: ERS scatterometer wind data impact on ECMWF's tropical cyclone forecasts. *IEEE Trans. Geosci. Remote Sens.*, **38**, 1885–1892, doi:10.1109/36.851771.

Jelenak, Z., P. S. Chang, J. M. Sienkeiwicz, and Q. Zhu, 2013: Hurricane force extratropical cyclones. *2012 Int. Ocean Vector Wind Science Team Meeting*, Kona, HI, NASA. [Available online at http://coaps.fsu.edu/scatterometry/meeting/docs/2013/Meteorology/zjelenak_HF_ETCs_IOVWST2013.pdf.]

Katsaros, K. B., P. W. Vachon, W. T. Liu, and P. G. Black, 2002: Microwave remote sensing of tropical cyclones from space. *J. Oceanogr.*, **58**, 137–151, doi:10.1023/A:1015884903180.

Kosaka, Y., 2014: Increasing wind sinks heat. *Nat. Climate Change*, **4**, 172–173, doi:10.1038/nclimate2138.

Liu, W. T., 2002: Progress in scatterometer application. *J. Oceanogr.*, **58**, 121–136, doi:10.1023/A:1015832919110.

——, W. Tang, and X. Xie, 2008: Wind power distribution over the ocean. *Geophys. Res. Lett.*, **35**, L13808, doi:10.1029/2008GL034172.

Lungu, T., and P. S. Callahan, Eds., 2006: QuikSCAT science data product user's manual: Overview and geophysical data products. Version 3.0, JPL Tech. Rep. D-18053-Rev A, 91 pp.

Martin, S., 2014: *An Introduction to Ocean Remote Sensing*. Cambridge University Press, 476 pp.

McPhaden, M. J., and Coauthors, 1998: The Tropical Ocean-Global Atmosphere observing system: A decade of progress. *J. Geophys. Res.*, **103**, 14 169–14 240, doi:10.1029/97JC02906.

——, and Coauthors, 2009: RAMA: The Research Moored Array for African-Asian-Australian Monsoon Analysis and Prediction. *Bull. Amer. Meteor. Soc.*, **90**, 459–480, doi:10.1175/2008BAMS2608.1.

Meissner, T., and F. J. Wentz, 2002: An updated analysis of the ocean surface wind direction signal in passive microwave brightness temperatures. *IEEE Trans. Geosci. Remote Sens.*, **40**, 1230–1240, doi:10.1109/TGRS.2002.800231.

——, and ——, 2006: Ocean retrievals for WindSat: Radiative transfer model, algorithm, validation. *2006 IEEE MicroRad Proceedings: 9th Specialist Meeting on Microwave Radiometry and Remote Sensing Applications*, IEEE. [Available online at http://images.remss.com/papers/rssconf/Meissner_microrad_2006_puertorico_windsat.pdf.]

——, and ——, 2009: Wind-vector retrievals under rain with passive satellite microwave radiometers. *IEEE Trans. Geosci. Remote Sens.*, **47**, 3065–3083, doi:10.1109/TGRS.2009.2027012.

——, and ——, 2012: The emissivity of the ocean surface between 6 and 90 GHz over a large range of wind speeds and Earth incidence angles. *IEEE Trans. Geosci. Remote Sens.*, **50**, 3004–3026, doi:10.1109/TGRS.2011.2179662.

——, ——, and L. Ricciardulli, 2014: The emission and scattering of L-band microwave radiation from rough ocean surfaces and wind speed measurements from the Aquarius sensor. *J. Geophys. Res. Oceans*, **119**, 6499–6522, doi:10.1002/2014JC009837.

National Research Council, 2004: *Climate Data Records from Environmental Satellites: Interim Report*. National Academies Press, 150 pp.

PMEL, 2013: TAO/TRITON sampling regimes. PMEL. [Available online at http://www.pmel.noaa.gov/tao/jsdisplay/help/help_data_sampling.html.]

Powell, M. D., S. H. Houston, L. R. Amat, and N. Morisseau-Leroy, 1998: The HRD real-time hurricane wind analysis system. *J. Wind Eng. Ind. Aerodyn.*, **77–78**, 53–64, doi:10.1016/S0167-6105(98)00131-7.

——, and Coauthors, 2010: Reconstruction of Hurricane Katrina's wind fields for storm surge and wave hindcasting. *Ocean Eng.*, **37**, 26–36, doi:10.1016/j.oceaneng.2009.08.014.

Renfrew, I. A., G. N. Peterson, D. A. J. Sproson, G. W. K. Moore, and H. Adiwidjaja, 2009: A comparison of aircraft-based surface-layer observations over Denmark Strait and the Irminger Sea with meteorological analyses and QuikSCAT winds. *Quart. J. Roy. Meteor. Soc.*, **135**, 2046–2066, doi:10.1002/qj.444.

Ricciardulli, L., and F. J. Wentz, 2011: Reprocessed QuikSCAT (V04) wind vectors with Ku-2011 geophysical model function. Remote Sensing Systems Tech. Rep. 043011, 8 pp. [Available online at http://images.remss.com/papers/rsstech/2011_043011_Ricciardulli_Qscat_Ku2011.pdf.]

——, and ——, 2012: Development of consistent geophysical model functions for different scatterometer missions: Ku and C-band. *2012 Int. Ocean Vector Wind Science Team Meeting*, Utrecht, Netherlands, NASA. [Available online at http://coaps.fsu.edu/scatterometry/meeting/docs/2012_meeting/New%20Products/Ricciardulli_IOVWST_2012_posted.pdf.]

——, and ——, 2013: Towards a climate data record of ocean vector winds: The new RSS ASCAT. *2013 Int. Ocean Vector Wind Science Team Meeting*, Kona, HI, NASA. [Available online at http://coaps.fsu.edu/scatterometry/meeting/docs/2013/New%20Products/Ricciardulli_ovwst_2013_ascat_winds_updated.pdf].

Roberts, J. B., C. A. Clayson, F. R. Robertson, and D. L. Jackson, 2010: Predicting near-surface atmospheric variables from special sensor microwave/imager using neural networks with a first-guess approach. *J. Geophys. Res.*, **115**, D19113, doi:10.1029/2009JD013099.

Robertson, F. R., M. G. Bosilovich, J. B. Roberts, R. H. Reichle, R. Adler, L. Ricciardulli, W. Berg, and G. J. Huffman, 2014: Consistency of estimated global water cycle variations over the satellite era. *J. Climate*, **27**, 6135–6154, doi:10.1175/JCLI-D-13-00384.1.

Stiles, B. W., and S. H. Yueh, 2002: Impact of rain on spaceborne Ku-band wind scatterometer data. *IEEE Trans. Geosci. Remote Sens.*, **40**, 1973–1983, doi:10.1109/TGRS.2002.803846.

Stoffelen, A., and D. Anderson, 1995: The ECMWF contribution to the characterization, interpretation, calibration and validation of ERS-1 scatterometer backscatter measurements and their use in numerical weather prediction models. ECMWF Contract Rep. 9097/90/NL/BI, 92 pp.

Tournadre, J., and Y. Quilfen, 2003: Impact of rain cell on scatterometer data: 1. Theory and modeling. *J. Geophys. Res.*, **108**, 3225, doi:10.1029/2002JC001428.

Uhlhorn, E. W., P. G. Black, J. L. Franklin, M. A. Goodberlet, J. R. Carswell, and A. S. Goldstein, 2007: Hurricane surface wind measurements from an operational stepped frequency microwave radiometer. *Mon. Wea. Rev.*, **135**, 3070–3085, doi:10.1175/MWR3454.1.

Verspeek, J., A. Stoffelen, M. Portabella, H. Bonekamp, C. Anderson, and J. Figa-Saldaña, 2010: Validation and calibration of ASCAT using CMOD5.n. *IEEE Trans. Geosci. Remote Sens.*, **48**, 386–395, doi:10.1109/TGRS.2009.2027896.

Weissman, D. E., and M. A. Bourassa, 2008: Measurements of the effect of rain-induced sea surface roughness on the QuikSCAT scatterometer radar cross section. *IEEE Trans. Geosci. Remote Sens.*, **46**, 2882–2894, doi:10.1109/TGRS.2008.2001032.

Wentz, F. J., 2013: SSM/I version-7 calibration report. Remote Sensing Systems Tech. Rep. 011012, 46 pp. [Available online at http://images.remss.com/papers/rsstech/2012_011012_Wentz_Version-7_SSMI_Calibration.pdf.]

——, and D. K. Smith, 1999: A model function for the ocean-normalized radar cross section at 14 GHz derived from NSCAT observations. *J. Geophys. Res.*, **104**, 11 499–11 514, doi:10.1029/98JC02148.

——, and L. Ricciardulli, 2011: Comment on "Global trends in wind speed and wave height." *Science*, **334**, 905, doi:10.1126/science.1210317.

——, V. J. Cardone, and L. S. Fedor, 1982: Intercomparison of wind speeds inferred by the SASS altimeter and SMMR. *J. Geophys. Res.*, **87**, 3378–3384, doi:10.1029/JC087iC05p03378.

——, L. A. Mattox, and S. Peteherych, 1986: New algorithms for microwave measurements of ocean winds: Applications to SeaSat and the Special Sensor Microwave Imager. *J. Geophys. Res.*, **91**, 2289–2307, doi:10.1029/JC091iC02p02289.

——, L. Ricciardulli, K. A. Hilburn, and C. A. Mears, 2007: How much more rain will global warming bring? *Science*, **317**, 233–235, doi:10.1126/science.1140746.

——, K. Hilburn, and T. Meissner, 2014: Two-look polarimetric (2LP) microwave radiometers for ocean vector wind retrieval. *2014 Int. Ocean Vector Wind Science Team Meeting*, Brest, France, NASA. [Available online at http://coaps.fsu.edu/scatterometry/meeting/docs/2014/OVWMissionUpdates/Wentz_IOVWST_2014_Brest3%20(2).pdf.]

Xie, S.-P., 2004: Satellite observations of cool ocean–atmosphere interaction. *Bull. Amer. Meteor. Soc.*, **85**, 195–208, doi:10.1175/BAMS-85-2-195.

Yu, L., and R. A. Weller, 2007: Objectively analyzed air–sea heat fluxes for the global ice-free oceans (1981–2005). *Bull. Amer. Meteor. Soc.*, **88**, 527–539, doi:10.1175/BAMS-88-4-527.

Yueh, S. H., and J. Chaubell, 2012: Sea surface salinity and wind retrieval using combined passive and active L-band microwave observations. *IEEE Trans. Geosci. Remote Sens.*, **50**, 1022–1032, doi:10.1109/TGRS.2011.2165075.

——, B. W. Stiles, and W. T. Liu, 2003: QuikSCAT wind retrievals for tropical cyclones. *IEEE Trans. Geosci. Remote Sens.*, **41**, 2616–2628, doi:10.1109/TGRS.2003.814913.